DOI: 10.1002/cmdc.200700208

Synthesis and Characterization of Cytidine Derivatives that Inhibit the Kinase IspE of the Non-Mevalonate Pathway for Isoprenoid Biosynthesis

Christine M. Crane,[a] Anna K. H. Hirsch,[a] Magnus S. Alphey,[b] Tanja Sgraja,[b] Susan Lauw,[c] Victoria Illarionova,[c] Felix Rohdich,*[c] Wolfgang Eisenreich,[c] William N. Hunter,*[b] Adelbert Bacher,[c] and François Diederich*[a]

The enzymes of the non-mevalonate pathway for isoprenoid biosynthesis are attractive targets for the development of novel drugs against malaria and tuberculosis. This pathway is used exclusively by the corresponding pathogens, but not by humans. A series of water-soluble, cytidine-based inhibitors that were originally designed for the fourth enzyme in the pathway, IspD, were shown to inhibit the subsequent enzyme, the kinase IspE (from Escherichia coli*). The binding mode of the inhibitors was verified by co-crystal structure analysis, using* Aquifex aeolicus *IspE. The crystal structures represent the first reported example of a co-crystal structure of IspE with a synthetic ligand and confirmed that ligand binding affinity originates mainly from the interactions of the nucleobase moiety in the cytidine binding pocket of the enzyme. In contrast, the appended benzimidazole moieties of the ligands adopt various orientations in the active site and establish only poor intermolecular contacts with the protein. Defined binding sites for sulfate ions and glycerol molecules, components in the crystallization buffer, near the well-conserved ATP-binding Gly-rich loop of IspE were observed. The crystal structures of* A. aeolicus *IspE nicely complement the one from* E. coli *IspE for use in structure-based design, namely by providing invaluable structural information for the design of inhibitors targeting IspE from* Mycobacterium tuberculosis *and* Plasmodium falciparum*. Similar to the enzymes from these pathogens,* A. aeolicus *IspE directs the OH group of a tyrosine residue into a pocket in the active site. In the* E. coli *enzyme, on the other hand, this pocket is lined by phenylalanine and has a more pronounced hydrophobic character.*

Introduction

The non-mevalonate pathway was discovered in the early 1990s in the research groups of Rohmer, Arigoni, and Sahm and uses seven enzymes in the assembly of the essential isoprenoid precursor molecules, isopentenyl diphosphate (IPP) and dimethylallyl diphosphate (DMAPP), starting from pyruvate and glyceraldehyde-3-phosphate (Scheme 1).[1] The pathway is used exclusively by many pathogens, such as the tuberculosis-causing *M. tuberculosis*[2] and the malaria-causing *P. falciparum*,[3,4] but not by humans. Taken together, tuberculosis[5] and malaria[6] are responsible for an estimated 300–500 million new infections and 3 million deaths annually. Efforts to combat these diseases are hampered by the rapid emergence of multidrug resistance in both organisms.[6,7]

Inhibition of the enzymes of the non-mevalonate pathway has been recognized as an alternative approach for the development of potential next-generation chemotherapeutics for the treatment of malaria and tuberculosis. Thus, Jomaa et al. showed that fosmidomycin [OHC–N(OH)–$(CH_2)_3$–PO_3H_2], a potent inhibitor of the second enzyme in the pathway, IspC (1-deoxy-D-xylulose-5-phosphate reductoisomerase, EC 1.1.1.267), cures malaria in rodents,[4] and this compound is being tested in clinical trials.[8]

A growing number of published X-ray crystal structures of the constituent enzymes of the non-mevalonate pathway have paved the way for the exploitation of these enzymes as targets in structure-based drug design.[9] If such a lead generation strategy focuses on several enzymes of the same biochemical pathway, chances increase for the identification of active ligands with the potential of inhibiting more than one enzyme

[a] *C. M. Crane, A. K. H. Hirsch, Prof. Dr. F. Diederich*
Laboratorium für Organische Chemie
ETH Zürich, HCI, CH-8093 Zürich (Switzerland)
Fax: (+41) 44-632-1109
E-mail: diederich@org.chem.ethz.ch

[b] *M. S. Alphey, T. Sgraja, Prof. Dr. W. N. Hunter*
Division of Biological Chemistry and Drug Discovery
College of Life Sciences, MSI/WTB Complex
University of Dundee, Dow Street Dundee DD1 5EH (UK)

[c] *S. Lauw, Dr. V. Illarionova, Dr. F. Rohdich, Dr. W. Eisenreich, Prof. Dr. A. Bacher*
Technische Universität München
Lehrstuhl für Organische Chemie und Biochemie
Lichtenbergstraße 4, 85748 Garching (Germany)

Supporting information for this article is available on the WWW under http://www.chemmedchem.org or from the author.

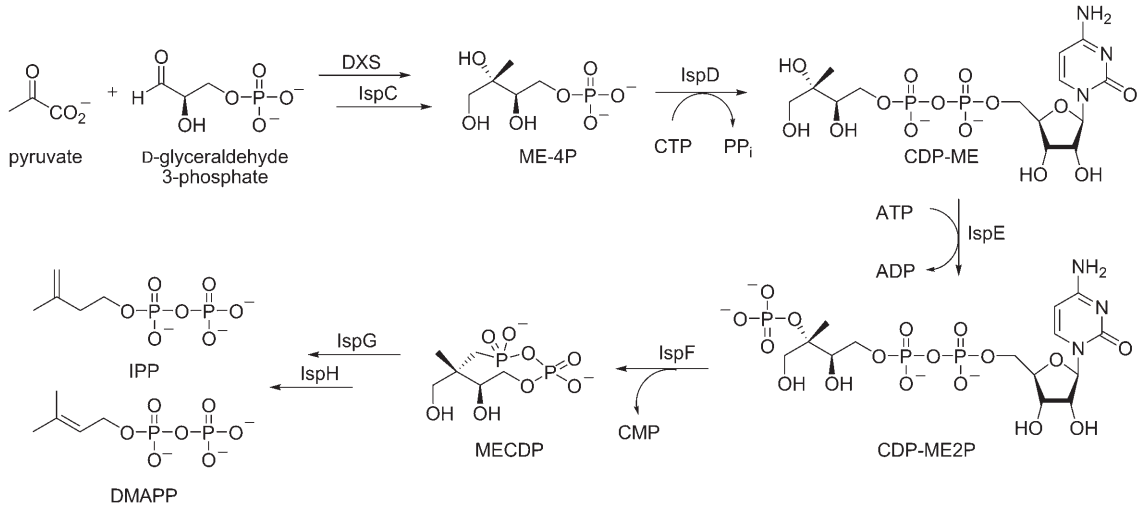

Scheme 1. The non-mevalonate pathway for the biosynthesis of the C_5 precursors to isoprenoids, IPP and DMAPP.[1] ADP = adenosine 5′-diphosphate, ATP = adenosine 5′-triphosphate, CDP-ME = 4-diphosphocytidyl-2*C*-methyl-D-erythritol, CDP-ME2P = 4-diphosphocytidyl-2*C*-methyl-D-erythritol-2-phosphate, DMAPP = dimethylallyl diphosphate, DXS = 1-deoxy-D-xylulose 5-phosphate synthase, IPP = isopentenyl diphosphate, MECDP = 2*C*-methyl-D-erythritol-2,4-cyclodiphosphate.

from this pathway, thereby generating valuable information on the binding modes of the various proteins. This article provides a strong example in support of such a "one-pathway-multi-target" strategy.

Our research group has focused on the structure-based design of inhibitors of two central enzymes in the pathway, IspE (4-diphosphocytidyl-2*C*-methyl-D-erythritol kinase, EC 2.7.1.148)[10] and IspF (2*C*-methyl-D-erythritol-2,4-cyclodiphosphate synthase, EC 4.6.1.12) (Scheme 1).[11] IspE is a kinase that catalyzes the phosphorylation of the 2-OH group of 4-diphosphocytidyl-2*C*-methyl-D-erythritol (CDP-ME), producing 4-diphosphocytidyl-2*C*-methyl-D-erythritol-2-phosphate (CDP-ME2P) in an ATP- and Mg^{2+}-dependent reaction (Scheme 1).[12] In the next step of the pathway, IspF catalyzes the cyclization of CDP-ME2P to the cyclic diphosphate 2*C*-methyl-D-erythritol-2,4-cyclodiphosphate (MECDP).[13] We found the development of low-molecular-weight, drug-like ligands very challenging: the enzymes feature highly polar active sites with limited concave hydrophobic surface, in accordance with the polar structures of their phosphate- and diphosphate-based substrates. Correspondingly, most inhibitors of enzymes in the pathway described in the literature feature phosphate or phosphonate moieties.[14] Only recently, we described more drug-like ligands for IspE and IspF that lack phosphate or phosphonate groups.[10,11b]

We also initially targeted the structure-based design of inhibitors for IspD (4-diphosphocytidyl-2*C*-methyl-D-erythritol-4-phosphate synthase, EC 2.7.7.60),[15] the enzyme that precedes IspE in the non-mevalonate pathway and catalyzes the transformation of 2*C*-methyl-D-erythritol-4-phosphate (ME-4P) into CDP-ME using cytidine 5′-triphosphate (CTP) and Mg^{2+} (Scheme 1). As part of these efforts, which were eventually discontinued, we prepared the series of water-soluble, cytidine-based derivatives (−)-**1**–(+)-**4** (Figure 1).

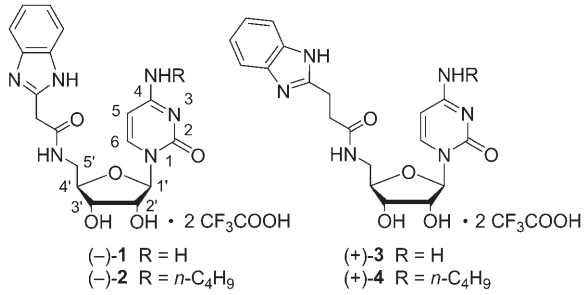

Figure 1. Cytidine derivatives investigated as inhibitors of IspE.

As IspE, similar to IspD, processes a cytidine-based substrate (Scheme 1),[13] the compounds were also tested against the kinase and shown to be moderately active inhibitors with K_i (inhibition constant) values in the double-digit micromolar range. Gratifyingly, the co-crystal structures of (−)-**1** and (+)-**3** bound to IspE from the thermophile *A. aeolicus* could be solved, and these structures revealed useful information for structure-based design efforts targeting IspE from other organisms such as *M. tuberculosis* and *P. falciparum*. Herein, we report the synthesis of the new ligands, their affinity towards IspE, and the co-crystal structures of (−)-**1** and (+)-**3** in complex with the kinase.

Results and Discussion

Synthesis of the inhibitors

The preparation of inhibitors (−)-**1**–(+)-**4** is shown in Schemes 2 and 3. The exocyclic NH_2 group of commercially available (+)-cytidine was N-acylated, and the 2′- and 3′-OH groups of the ribose moiety were protected as an acetonide, affording (−)-**5**. Mitsunobu reaction with phthalimide, using

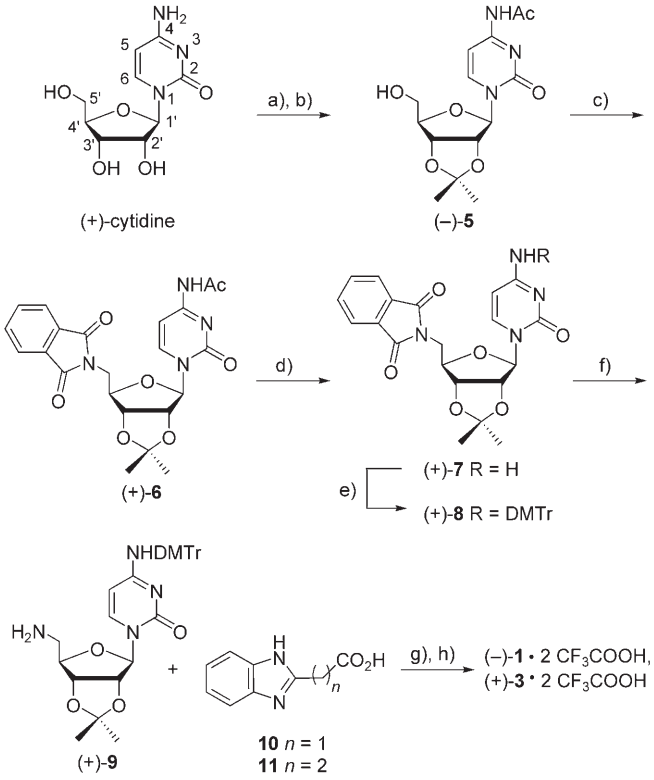

Scheme 2. Synthesis of inhibitors (−)-**1** and (+)-**3**. a) Ac_2O, MeOH, 75 °C→20 °C, 18 h, 90%; b) $HC(OEt)_3$, *p*-TsOH, acetone, 20 °C, 1 h, 83%; c) Phthalimide, Ph_3P, DIAD, DMF, 20 °C, 18 h, 70%; d) 7 N NH_3 in MeOH, CH_2Cl_2/MeOH 1:1, 20 °C, 6 h, 85%; e) Et_3N, DMTrCl, CH_2Cl_2, 20 °C, 1 h, 85%; f) $nBuNH_2$, EtOH, 60 °C, 5 h, 87%; g) **10** or **11**, HBTU, HOBt, Et_3N, DMF, 0 °C→20 °C, 18 h; h) TFA, CH_3CN/H_2O, 20 °C, 2 h, (−)-**1** (31%), (+)-**3** (51%). DIAD = diisopropyl azodicarboxylate, DMF = *N*,*N*-dimethylformamide, DMTrCl = dimethoxytrityl chloride, HBTU = *O*-benzotriazole-*N*,*N*,*N*′,*N*′-tetramethyluronium hexafluorophosphate, HOBt = 1-hydroxybenzotriazole, Ph = phenyl, TFA = trifluoroacetic acid, Ts = toluenesulfonyl.

diisopropyl azodicarboxylate and triphenylphosphine in *N*,*N*-dimethylformamide, afforded intermediate (+)-**6** in good yield. At this stage of the synthesis, it became necessary to convert the acetyl into a more stable N-protecting group, as it was found to react under the conditions of phthalimide cleavage, which typically employs nucleophilic bases such as hydrazine, methylamine, or *n*-butylamine. These bases can attack both the acetamido moiety as well as the adjacent C4 of N-acetylated cytosines (for atom labeling, see Scheme 2) to afford mixtures of products.[16] Deacetylation of (+)-**6** was successful with the use of ammonia in methanol/dichloromethane and afforded cytidine derivative (+)-**7** in good yield. The 4,4′-dimethoxytrityl group (DMTr, bis(4-methoxyphenyl)(phenyl)methyl) was found to be the most suitable protecting group for the exocyclic NH_2 group, as it effectively prevented nucleophilic attack at C4 of cytosine. Subsequent reaction of (+)-**7** with 4,4′-dimethoxytrityl chloride and triethylamine in dichloromethane afforded (+)-**8** in 85% yield. The phthalimide moiety was subsequently transformed into primary amine (+)-**9** in 87% yield by using *n*-butylamine in methanol at 60 °C. Coupling of (+)-**9** with 1*H*-benzimidazol-2-yl-acetic acid (**10**)[17] or commercially available 2-benzimidazolepropionic acid (**11**), using *O*-benzotriazole-*N*,*N*,*N*′,*N*′-tetramethyluronium hexafluorophosphate (HBTU), 1-hydroxybenzotriazole (HOBt), and triethylamine, followed by acetonide and DMTr deprotection using 30% trifluoroacetic acid in acetonitrile/water afforded (−)-**1** and (+)-**3** as bis(trifluoroacetate) salts (Scheme 2).

Interestingly, the ^{1}H NMR spectra of (+)-**8** in CD_3OD and (+)-**9** in $CDCl_3$ recorded at 298 K showed the presence of two conformers (Supporting Information Figures 1SI and 2SI, and Tables 1SI and 2SI). In particular, the cytosine resonances of H–C5 and H–C6 of (+)-**8** and (+)-**9** differ strongly in the two conformations (arbitrarily labeled **A** and **B**). The observation of the conformational equilibrium is strongly solvent dependent (see Supporting Information). The origin of the conformers, be it from rotation about the C4–N_{exo} bond (*cis*/*trans*) or the glycosidic bond (*syn*/*anti*), as well as their structural assignment and the thermodynamics and kinetics of the equilibrium, are under further investigation.

The *N*-butyl derivatives (−)-**2** and (+)-**4** were obtained starting from *tert*-butylcarbamate-protected (+)-**12** (Scheme 3),

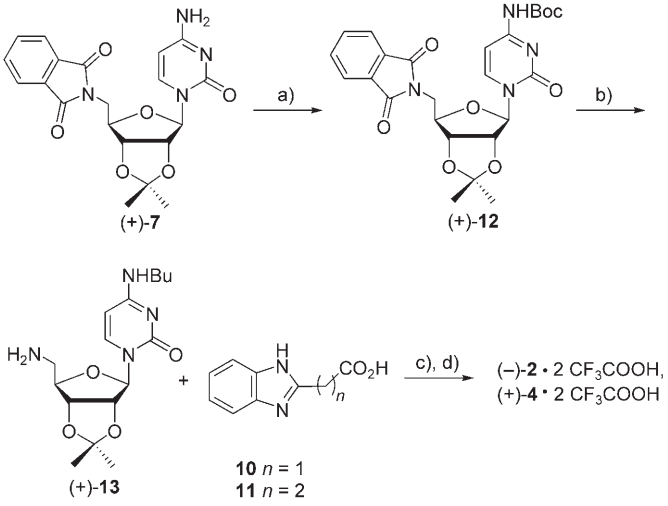

Scheme 3. Synthesis of cytidine derivatives (−)-**2** and (+)-**4**. a) Boc_2O, dioxane/THF, 70 °C, 6 h, 90%; b) i) $nBuNH_2$, EtOH, 70 °C, 6 h, ii) 75 °C, 2 h, 82%; c) **10** or **11**, HBTU, HOBt, Et_3N, DMF, 0 °C→20 °C, 18 h; d) TFA, CH_3CN/H_2O, 20 °C, 2 h, (−)-**2** (29%), (+)-**4** (39%). Boc = *t*-butyloxycarbonyl.

which in turn was formed in excellent yield by protecting (+)-**7** with di-*tert*-butylcarbonate in dioxane/tetrahydrofuran at 70 °C. Surprisingly, cleavage of the phthalimide, using *n*-butylamine in ethanol at 70 °C, provided (+)-**13** in 80% yield. As mentioned above, similar conversions have been noted to occur on N-acetylated cytidines,[16] but always as minor side reactions. N-Butylated (+)-**13** was immediately used after preparation, as it was found to rapidly decompose, even at −20 °C. Coupling with **10** or **11** in the presence of HBTU, HOBt, and triethylamine, followed by acetonide deprotection using 30% trifluoroacetic acid in acetonitrile/water, afforded (−)-**2** and (+)-**4** as the bis-trifluoroacetate salts. Again, the ^{1}H NMR spectra at 298 K revealed the presence of two isomers (Supporting Information Figures 3SI and 4SI).

Biological results

The IC_{50} values (IC_{50} = concentration of inhibitor at which 50% maximum initial velocity is observed) for (−)-**1**–(+)-**4** were determined using a photometric assay employing a complex set of auxiliary enzymes and *E. coli* IspE (Table 1 and Supporting Information Figure 5SI).[18] Whereas cytidine derivatives (−)-**1** and (+)-**3** were found to inhibit the kinase, the *N*-butyl derivatives (−)-**2** and (+)-**4** were found to be completely inactive. Inhibition of the IspE-catalyzed reaction by ligands (−)-**1** and (+)-**3** was independently confirmed in an enzymatic assay monitoring the phosphorylation of the substrate [1,3,4-$^{13}C_3$]CDP-ME (1 mM) by ^{13}C NMR spectroscopy. The inhibitory mechanisms for (−)-**1** and (+)-**3** were subsequently determined, and evaluation of the data using the computer program Dynafit[19] revealed fully competitive inhibition, with K_i values in the upper double-digit micromolar range (Table 1 and Supporting Information Figure 6SI).

Table 1. Biological activities of cytidine derivatives (−)-**1**–(+)-**4** against *E. coli* IspE.

Compound	K_i [μM][a]	IC_{50} [mM][b]
(−)-**1**	85.8 ± 9.4	1.99
(−)-**2**	–[c]	inactive[d]
(+)-**3**	71.2 ± 6.2	1.67
(+)-**4**	–[c]	inactive[d]

[a] K_i = competitive inhibition constant. [b] IC_{50} values were determined at [CDP-ME] = 1 mM. [c] Not determined. [d] No inhibition of the IspE-catalyzed reaction observed at [inhibitor] = 2 mM.

Prior to this work, two X-ray crystal structures of IspE were available, one from the apo-enzyme of *Thermus thermophilus* (1.7 Å resolution, RCSB Protein Data Bank (PDB) code: 1UEK),[20] and the other from the ternary complex of *E. coli* IspE bound to CDP-ME and 5′-adenyl-β,γ-amidotriphosphate (AppNp), a non-hydrolyzable ATP analogue (2.0 Å resolution, PDB code: 1JO4, Supporting Information Figure 7SI).[21] The structures revealed that IspE contains three main binding pockets: the adenosine binding, the cytidine binding, and the 2*C*-methyl-D-erythritol-2-phosphate (MEP) binding pockets (Supporting Information Figure 7SI). The fact that (−)-**1** and (+)-**3** are competitive inhibitors with respect to the substrate indicates that the cytidine moiety is probably located in the homonymous pocket, in agreement with molecular modeling predictions using the program MOLOC.[22] This pocket does not provide space to accommodate the butyl substituent on the exocyclic amino group of the nucleobase, and this explains the lack of binding of (−)-**2** and (+)-**4**. Furthermore, the weak affinity suggests that little if any binding free enthalpy is gained from the benzimidazole component and that the majority of the affinity may indeed come from the nucleobase. The benzimidazole moiety is far too large to occupy the small, hydrophobic subpocket near the MEP binding pocket, which was more optimally filled with smaller residues such as cyclopropyl rings, with a substantial gain in binding free enthalpy.[10] On the other hand, we detected no binding of cytidine, CMP, CDP, or CTP within the limits of our assay. To verify these hypotheses and to further investigate the binding modes of inhibitors (−)-**1** and (+)-**3**, X-ray crystallographic studies of co-crystals were undertaken.

X-ray crystallography

Two crystal structures of IspE have been reported,[20,21] however it is difficult to obtain crystals with these proteins for ligand binding studies. The enzyme from *A. aeolicus* has been found to be more reliable in this respect and provided co-crystals with (−)-**1** and (+)-**3** suitable for X-ray analysis.

The structures of complexes of (−)-**1** (Figure 2 and Supporting Information Figure 8SI) and (+)-**3** (Supporting Information Figures 9SI and 10SI) with *A. aeolicus* IspE were determined to 2.4 Å and 2.3 Å resolution, respectively. The complexes are isomorphous and contain two molecules in the asymmetric unit that are related by a non-crystallographic twofold axis. The surface area between the two molecules is approximately 540 $Å^2$ per molecule, only 4% of the total surface area of the protein. This low value is consistent with gel filtration and ultracentrifugation experiments (data not shown) that indicate the enzyme is a monomer in solution.[24] Overall, the secondary structure of *A. aeolicus* IspE is similar to that of *E. coli*[21] and *T. thermophilus* IspE.[20]

The complexes of (−)-**1** and (+)-**3** with *A. aeolicus* IspE confirm that the cytidine moieties of both inhibitors are held in the cytidine binding pocket, as suggested by molecular modeling[22] of these inhibitors docked into the active site of *E. coli* IspE. In the solved X-ray crystal structures, the cytosine base is H bonded to the side chain and backbone of His 25 and the backbone carbonyl of Lys 145. In addition, it is placed at the center of a π sandwich made of Tyr 24 and Tyr 175 (see Figure 2a and Supporting Information Figure 9SI). The presence of a second H bond between the exocyclic amine of the cytosine and the backbone carbonyl of Lys 145 in *A. aeolicus* IspE explains the absence of inhibitory activity of compounds (−)-**2** and (+)-**4** (Figure 1). The butyl chain at this position prevents formation of this H bond and leads to steric clashes with residues in this region of the active site, rather than providing additional hydrophobic contacts. Unlike the nucleobase, the ribose moiety of the ligands is not involved in strong interactions with the active site residues.

The independent views of the active site in the complex with (−)-**1** reveal two conformations of the benzimidazole moiety, neither of which is well ordered. The group does not occupy the MEP binding pocket (Figure 2b) or the adenosine binding pocket (Figure 2c). Furthermore, the benzimidazole moiety in active site A (Figure 2) does not adopt exactly the same conformation as that observed in active site B (Supporting Information Figure 8SI). The lack of order and observation of different conformations for this part of the ligands may indicate a lack of specificity, and further suggest this group probably does not contribute significantly to binding affinity.

In the complex with (+)-**3**, the benzimidazole moiety is not involved in any additional interactions that could explain its

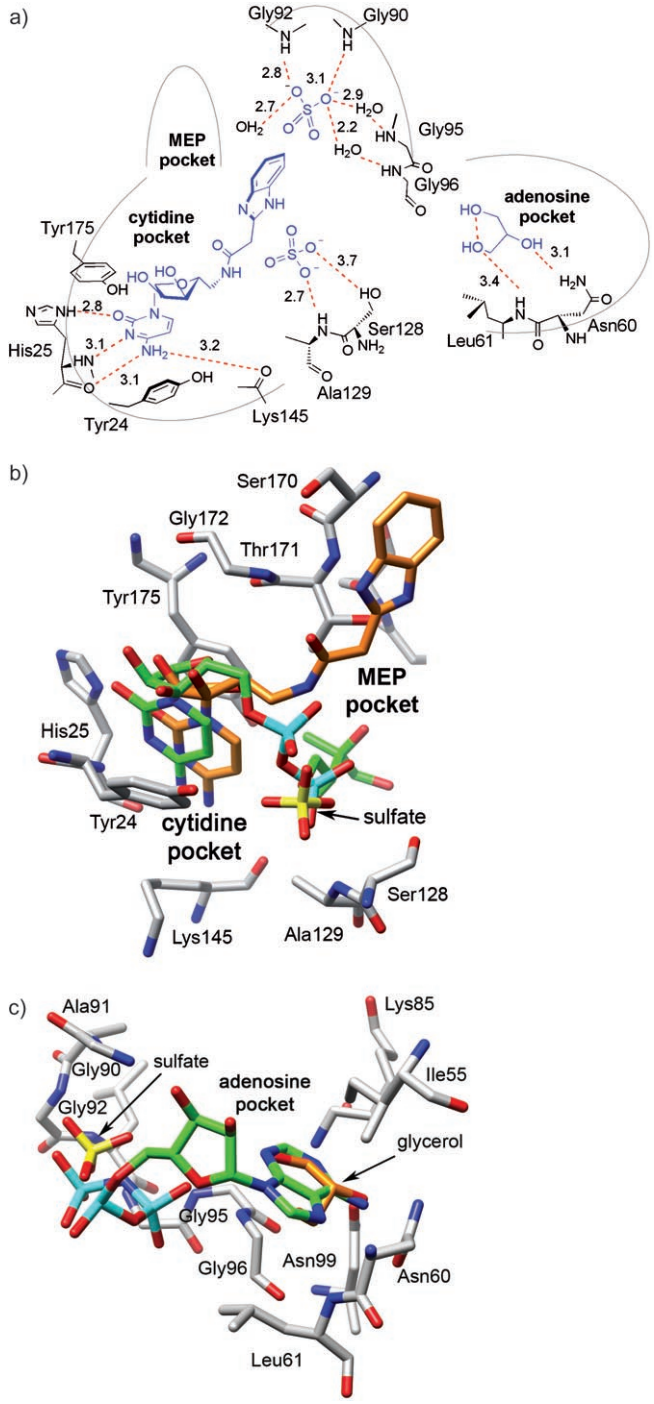

Figure 2. Binding mode of inhibitor (−)-**1** in the active site of *A. aeolicus* IspE (PDB code: 2V2Q) as determined by X-ray crystallography to 2.4 Å resolution. a) Schematic representation of the binding mode of (−)-**1** as observed in active site A. H bonds are represented as red dashed lines. Distances between heavy atoms are given in Å. b) Superposition of CDP-ME as observed in active site A of *E. coli* IspE (PDB code: 1OJ4)[21] onto (−)-**1** as observed in active site A of *A. aeolicus* IspE. The sulfate ion is in the position of the β-phosphate of CDP-ME, and the benzimidazole moiety is oriented out of the MEP pocket. c) Superposition of AppNp, as observed in active site A of *E. coli* IspE (PDB code: 1JO4)[21] onto (−)-**1** as observed in active site A of *A. aeolicus* IspE. The glycerol is located near the adenine binding region of the active site. Color code: substrate skeleton: C: green; inhibitor skeleton: C: orange; protein skeleton: C: grey; O: red; N: blue; S: yellow; P: cyan. All figures were generated with the molecular graphics program Chimera.[23]

marginally higher affinity relative to inhibitor (−)-**1** (Table 1). Again, the benzimidazole moiety occupies two very different locations in the active site, neither in the MEP nor in the adenine binding pockets, and is poorly ordered. In active site A, the benzimidazole is near residues Ser 170–Thr 171 (Supporting Information Figure 9SI) and in active site B it appears to adopt an almost collapsed conformation, with the benzimidazole moiety near residues Ala 129 and Asp 130 (Supporting Information Figure 10SI).

Ammonium sulfate ($(NH_4)_2SO_4$) and glycerol were required for co-crystallization of the inhibitors and the protein. As they were not added under the enzyme assay conditions, they are not thought to be required for binding of the inhibitors. Both crystal structures contain a number of sulfate ions in the two active sites, providing valuable structural information on the recognition of these anions (described in detail in the Supporting Information, Figures 8SI–10SI).[25]

The presence of these sulfate ions in the P-loop, usually used to accommodate the much larger triphosphate moiety of ATP, indicates that the loop is generally well organized, even in the absence of ATP or an ATP analogue. The knowledge gained on the pre-organization of this phosphate binding loop could be exploited in second-generation inhibitors by directing fragments with multiple H-bond acceptor sites into the loop, as proposed previously.[26]

Comparisons of IspE from different organisms

The two protein–inhibitor co-crystal structures revealed three important insights. First, the benzimidazole moiety of the ligands is poorly ordered in the active site. This suggests only a minor contribution to the binding free enthalpy. Second, the cytidine binding pocket and its interactions with the nucleobase are highly conserved. Finally, the Gly-rich P-loop involved in cofactor binding seems to be well conserved and well ordered, even in the absence of ATP or an ATP analogue.

To date, the ternary complex of *E. coli* IspE has been successfully used for modeling, producing the first inhibitors of IspE from this organism.[10] However, small structural differences between the enzyme of the *E. coli* model system and the enzyme of the targeted organisms, that is, *M. tuberculosis* and *P. falciparum*, became apparent upon examination of the *A. aeolicus* IspE complexes with inhibitors (−)-**1** and (+)-**3**. A detailed comparison of the *E. coli* and *A. aeolicus* IspE structures will be reported elsewhere, although at this stage, we would like to point out that in terms of substrate and co-factor binding, the two enzymes are highly similar.[24] It was deemed crucial, for ongoing projects, to compare the active site residues among the *M. tuberculosis*, *P. falciparum*, *A. aeolicus*, and *E. coli* homologues, specifically focusing on the small, hydrophobic pocket filled by cyclopropyl and similarly sized residues in the first-generation *E. coli* IspE inhibitors.[10] The comparison revealed that in general the overall architecture of the active site is likely well conserved across the different organisms, with the exception of a few, but important, variations in active site amino acid residues (for a sequence alignment of IspE homo-

logues from several organisms, see Supporting Information Figure 11SI).

A simplified comparison of the active site residues of IspE from *M. tuberculosis*, *P. falciparum*, *A. aeolicus*, and *E. coli* is depicted in Figure 3. As expected, the important catalytically active residues Lys 10 and Asp 141 in the MEP pocket, are fully conserved among the various organisms (Figure 3 a), however this trend changes in the cytidine pocket. In *E. coli* IspE, the cytosine base H bonds to the backbone and side chain of His 26. While in *M. tuberculosis* and *A. aeolicus* IspE nucleobase recognition is also achieved by His, in *P. falciparum*, this amino acid is replaced by Asn, which can be considered an isosteric replacement. The ribose moiety of the substrate in *E. coli* IspE is anchored by H bonding to Lys 186 and by hydrophobic interactions through its positioning at the center of a pseudo π sandwich composed of Tyr 25 and Pro 182. Whereas the tyrosine residue is widely conserved among the various organisms, the Pro residue is replaced by Lys (*P. falciparum*), Ser (*M. tuberculosis*), or Gly (*A. aeolicus*) (Figure 3 a and Supporting Information Figure 11bSI). Additional stabilization of the substrate in the *E. coli* protein is derived from placing the cytosine at the center of a π sandwich formed by the highly conserved aromatic amino acids Tyr 25 and Phe 185.[10] The small hydrophobic pocket in *E. coli* IspE, which was successfully filled by the first-generation inhibitors (with K_i values down to the upper nanomolar range),[10] is lined by Leu 15, Leu 28, and Phe 185, the latter of which is engaged in the π sandwich described above. While Leu 15 is fully conserved among the various organisms, Leu 28 is conserved in *M. tuberculosis*, but replaced by Val in *P. falciparum* or Ile in *A. aeolicus*, both of which can be considered to be of similar steric demand (Figure 3 a and Supporting Information Figure 11aSI). On the other hand, replacement of the highly hydrophobic Phe 185 in *E. coli* IspE with a more hydrophilic tyrosine residue in *M. tuberculosis*, *P. falciparum*, and *A. aeolicus* (Figure 3 a and Supporting Information Figure 11bSI) should affect the binding characteristics of this pocket. In the structures of the complexes of *A. aeolicus* reported herein, the OH group of tyrosine points directly into this small pocket, thereby strongly decreasing its hydrophobic character. This important observation could assist future rounds of design and synthesis to improve on the first-generation inhibitors, especially with regard to their activity against the targeted IspE proteins from *M. tuberculosis* and *P. falciparum*.

Conclusions

We have reported the synthesis, in vitro evaluation, and co-crystal structures of two fully water-soluble nucleoside-based inhibitors of IspE. Biological assays revealed competitive inhibition of *E. coli* IspE with K_i values in the upper double-digit micromolar range. The presumed binding modes of the nucleobase portion of (−)-**1** and (+)-**3** were largely confirmed by analysis of co-crystal structures obtained with *A. aeolicus* IspE, a protein that seems to lend itself well to protein–ligand co-crystallization. These first reported co-crystal structures of IspE with synthetic ligands suggest that the majority, if not all, of the affinity of the ligands for IspE is derived from the cytidine portion. The benzimidazole moiety is poorly ordered and can adopt different orientations, with poor intermolecular contacts in the active site, thereby making only a small contribution to the binding affinity. The crystal structures revealed defined binding sites for sulfate ions and glycerol molecules, used as components in the crystallization buffer, near the well-conserved ATP binding Gly-rich loop of IspE. We intend to exploit this loop for gaining additional docking interactions with next-

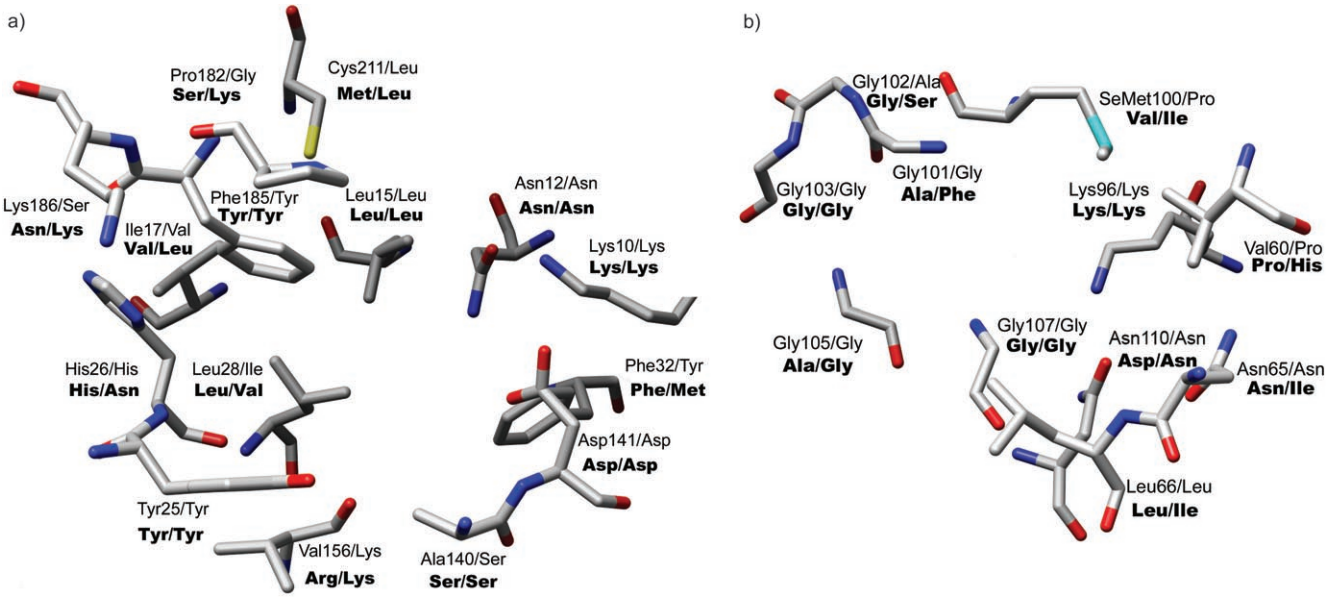

Figure 3. A comparison of the key amino acid residues of *E. coli* IspE (PDB code: 1JO4;[21] left non-bolded) with those of IspE from *A. aeolicus* (right non-bolded), *M. tuberculosis* (left bold), and *P. falciparum* (right bold) in a) cytidine and MEP binding pockets and b) adenosine binding pocket. Numbering is according to *E. coli* IspE protein.

generation inhibitors. For our work targeting the inhibition of IspE from *P. falciparum* and *M. tuberculosis*, it was important to find that an OH group of a tyrosine side chain of *A. aeolicus* IspE is directed into the small hydrophobic cavity. This is the same hydrophobic cavity that we had filled with cyclopropyl and related residues in our first-generation inhibitors of *E. coli* IspE, in which this tyrosine is replaced with phenylalanine.[10] A comparison among various organisms showed that IspE from *P. falciparum* and *M. tuberculosis*, similar to *A. aeolicus*, also features a tyrosine directing the OH group into the small pocket. Therefore, the presented structures of *A. aeolicus* IspE should be particularly useful for future structure-based lead design targeting the parasite enzymes.

Experimental Section

General. *N*-Acetylcytidine[27] and **10**[17] were prepared according to published procedures. Reagents and solvents were purchased reagent-grade and used without further purification. (+)-Cytidine was purchased from Acros Organics, and 2-benzimidazolepropionic acid (**11**), from Aldrich. THF was freshly distilled from sodium benzophenone ketyl. All reactions were performed in oven-dried glassware under N_2 atmosphere unless otherwise stated. Evaporation and concentration in vacuo were performed at $\leq 40\,^{\circ}C$ and ~10 Torr. Further drying of the new compounds was carried out at $\sim 10^{-2}$ Torr. TLC: pre-coated SiO_2 60 F_{254} glass plates from Merck, visualization by UV light (254 or 366 nm) or by staining with a solution of ninhydrin. Flash chromatography (FC): SiO_2 60 (0.04–0.063 mm) from Fluka with a head pressure of ~0.2 bar. Analytical HPLC was performed on a Knauer Prontosil 120 C_{18} column (259× 4 mm, 5 μm, 100 Å); products were eluted with CH_3CN in H_2O containing 0.1% TFA at a flow rate of 1 mL min^{-1} and with UV detection at $\lambda = 254$ nm. Preparative HPLC was performed on a Knauer Prontosil 120-5 C_{18} column (250×25 mm, 7 μm, 100 Å); products were eluted with CH_3CN in H_2O containing 0.1% TFA at a flow rate of 10 mL min^{-1} and with UV detection at $\lambda = 254$ nm. Uncorrected melting points (mp) were determined in an open capillary using a Büchi Melting Point B540 apparatus. NMR (^{1}H or ^{13}C): Bruker AMX-II 500, Bruker AMX-II 300, Varian Mercury XL, or Gemini 300 NMR spectrophotometers at 298 K. Residual solvent peaks were used as an internal reference. Coupling constants (*J*) (H,H) are given in Hz. Coupling patterns are designated as singlet (s), doublet (d), triplet (t), quadruplet (q), quintuplet (qt), multiplet (m), or broad signal (br). IR spectra: PerkinElmer 1600-FTIR or PerkinElmer Spectrum BX FT-IR spectrophotometer, measured as a film (NaCl plates) or neat. FT-ICR-MALDI-MS: Ion Spec Ultima FT-ICR-MS (337 nm N_2 laser system). Matrix: 3-HPA (3-hydroxypicolinic acid); the detected masses are given as *m/z* with *M* representing the molecular ion. Elemental analyses were performed by the Mikrolabor at the Laboratorium für Organische Chemie, ETH Zürich. Cytidine moieties are labeled according to convention; for the arbitrary labeling of residual molecular fragments, see Supporting Information Figure 12SI.

General procedure A for coupling reactions: A solution of the amine (1.0 equiv) and Et_3N (1.0 equiv) in anhydrous DMF (0.15 M) was added dropwise to a stirred solution of the corresponding acid (1.0 equiv), HOBt (1.0 equiv), and HBTU (1.0 equiv) in anhydrous DMF (0.1 M) at 20 °C. After 18 h, the volatiles were removed in vacuo, and the residue was purified by FC. The protected intermediates were carried through to the next step according to general procedure B without further characterization.

General procedure B for removal of protecting groups: TFA (30%) was added dropwise to a stirred solution of the products obtained from general procedure A in CH_3CN/H_2O 1:1 at 20 °C. After 2 h, the volatiles were removed in vacuo, and the crude residue was purified by reversed-phase (RP) HPLC (see the experimental details).

2-[2-({[(2*R*,3*S*,4*R*,5*R*)-5-(4-Ammonio-2-oxopyrimidin-1(2*H*)-yl)-3,4-dihydroxytetrahydrofuran-2-yl]methyl}amino)-2-oxoethyl]-1*H*-3,1-benzimidazol-1-ium bis(trifluoroacetate) ((−)-**1**): General procedure A, starting from the amine (+)-**9** (117 mg, 0.20 mmol) and Et_3N (28 μL, 0.20 mmol) in anhydrous DMF (1.6 mL) and **10**[17] (35 mg, 0.20 mmol), HOBt (28 mg, 0.20 mmol), and HBTU (78 mg, 0.20 mmol) in anhydrous DMF (1.60 mL). FC (Et_3N/MeOH/AcOEt 1:10:89) afforded the protected intermediate (36 mg, 47%), which was taken directly to the next step without further characterization. General procedure B, starting from this intermediate and TFA (0.50 mL) in CH_3CN/H_2O 1:1 (1.6 mL). RP HPLC (1:99 (10 min)→35:65 (20 min)→100%, H_2O with 0.1% TFA/CH_3CN), followed by lyophilization of the aqueous phases afforded the bis-TFA salt of (−)-**1** (38.6 mg, 31% over two steps). White powder; mp: 144–145 °C; $[\alpha]_D^{20} = -1.6$ (*c* = 0.5, MeOH); ^{1}H NMR (300 MHz, CD_3OD): $\delta =$ 2.66 (s, 2H, H-C8), 3.60 (dd, *J* = 13.8, 2.4 Hz, 1H, H_a-C5′), 3.67 (dd, *J* = 13.8, 6.3 Hz, 1H, H_b-C5′), 4.03–4.08 (m, 2H, H-C3′ and H-C4′), 4.26–4.31 (m, 1H, H-C2′), 5.69 (d, *J* = 3.6 Hz, 1H, H-C1′), 6.10 (d, *J* = 7.8 Hz, 1H, H-C5), 7.56–7.61 (m, 2H, H-C13), 7.75–7.81 (m, 2H, H-C12), 8.02 ppm (d, *J* = 7.8 Hz, 1H, H-C6); ^{13}C NMR (75 MHz, CD_3OD): $\delta =$ 42.21 (C8), 43.84 (C5′), 72.04 (C3′), 74.07 (C2′), 83.80 (C4′), 94.41 (C1′), 94.78 (C5), 114.66 (C12), 127.27 (C13), 132.14 (C11), 147.06 (C6), 148.62 (C2), 148.92 (C9), 161.38 (C4), 166.85 ppm (C7); IR (neat): $\tilde{\nu} =$ 3251w, 3075w, 2930w, 2777w, 1663s (br), 1561w, 1540w, 1460w, 1425w, 1297w, 1261w, 1184s (br), 1130s (br), 1070w, 944w, 887w, 834m, 798 m, 750m, 721s cm^{-1}; HR-MALDI-MS (3-HPA): calcd for $C_{18}H_{21}N_6O_5^+$ ([*M*+H]$^+$): 401.1568, found: 401.1561.

2-{2-[({(2*R*,3*S*,4*R*,5*R*)-5-[4-(Butylammonio)-2-oxopyrimidin-1(2*H*)-yl]-3,4-dihydroxytetrahydrofuran-2-yl}methyl)amino]-2-oxoethyl}-1*H*-3,1-benzimidazol-1-ium bis(trifluoroacetate) ((−)-**2**): General procedure A, starting from amine (+)-**13** (50 mg, 0.15 mmol) and Et_3N (21 μL, 0.15 mmol) in anhydrous DMF (1 mL) and **10**[17] (26 mg, 0.15 mmol), HBTU (56 mg, 0.15 mmol), and HOBt (20 mg, 0.15 mmol) in anhydrous DMF (1.5 mL). FC (Et_3N/MeOH/AcOEt 1:10:89) afforded the protected intermediate (28.5 mg, 38%), which was taken directly to the next step without further characterization. General procedure B, starting from this intermediate and TFA (0.37 mL) in CH_3CN/H_2O (1:1, 1.2 mL). RP HPLC (5:95 (10 min)→35:65 (20 min)→100% H_2O with 0.1% TFA/CH_3CN), followed by lyophilization of the aqueous phases afforded the bis-TFA salt of (−)-**2** (29.6 mg, 29% over two steps) as a mixture of two conformers denoted **A** and **B** (CD_3OD, **A**/**B** = 3:1). White powder; mp: > 128 °C (dec); $[\alpha]_D^{20} = -17.5$ (*c* = 0.5, MeOH); ^{1}H NMR (300 MHz, CD_3OD): $\delta =$ 0.97 (t, *J* = 7.2 Hz, 6H, H-C10), 1.37–1.49 (m, 4H, H-C9), 1.65 (qt, *J* = 7.2 Hz, 4H, H-C8), 3.40 (t, *J* = 7.2 Hz, 4H, H-C7), 3.60–3.75 (m, 4H, H-C5′), 4.02–4.10 (m, 4H, H-C3′ and H-C4′), 4.27–4.34 (m, 2H, H-C2′), 5.65 (d, *J* = 3.0 Hz, 1H, H_B-C1′), 5.70 (d, *J* = 3.8 Hz, 1H, H_A-C1′), 6.05 (d, *J* = 7.8 Hz, 1H, H_A-C5), 6.29 (d, *J* = 8.1 Hz, 1H, H_B-C5), 7.55–7.61 (m, 4H, H-C17), 7.75–7.80 (m, 4H, H-C16), 7.83 (d, *J* = 7.8 Hz, 1H, H_A-C6), 8.08 ppm (d, *J* = 8.1 Hz, 1H, H_B-C6); ^{13}C NMR (125 MHz, CD_3OD): $\delta =$ 13.89 (C_B10), 13.92 (C_A10), 20.77 (C_B9), 20.94 (C_A9), 31.34 (C_A8), 31.86 (C_B8), 42.22 (C_B7), 42.61 (C5′), 43.11 (C_A7), 44.16 (C12), 72.14 (C_B3′), 72.42 (C_A3′), 74.87 (C_A2′), 74.94 (C_B2′), 83.82 (C_A4′), 84.08 (C_B4′), 92.01 (C_B1′), 95.56 (C_A1′), 96.26 (C_A5), 95.36 (C_B5), 114.91 (C16), 127.38 (C17), 132.57 (C15), 144.14 (C6), 148.22 (C13), 149.21 (C_A2), 151.92 (C_B2), 160.63 (C_B4), 160.87 (C_A4),

167.10 ppm (C11), (14 C signals buried); IR (neat): $\tilde{\nu}$ = 3261w, 3070w, 2935w, 2868w, 1734w, 1670s (br), 1590s (br), 1459w, 1430w, 1347w, 1277w, 1199s (br), 1131s (br), 1073m, 944w, 833m, 798m, 750 m, 721s cm^{-1}; HR-MALDI-MS (3-HPA): calcd for $C_{22}H_{29}N_6O_5^+$ ($[M+H]^+$): 457.2194, found: 457.2188.

1-[(2*R*,3*R*,4*S*,5*R*)-5-({[3-(1*H*-Benzimidazol-3-ium-2-yl)propanoyl]amino}methyl)-3,4-dihydroxytetrahydrofuran-2-yl]-2-oxo-1,2-dihydropyrimidin-4-aminium bis(trifluoroacetate) ((+)-**3**): General procedure A, starting from the amine (+)-**9** (88 mg, 0.15 mmol) and Et_3N (21 μL, 0.15 mmol) in anhydrous DMF (1 mL) and commercially available **11** (28 mg, 0.15 mmol), HBTU (56 mg, 0.15 mmol), and HOBt (20 mg, 0.15 mmol) in anhydrous DMF (1.5 mL). FC (Et_3N/MeOH/AcOEt 1:10:89) afforded the protected intermediate (97.7 mg, 86%), which was taken directly to the next step without further characterization. General procedure B, starting from this intermediate and TFA (0.74 mL) in CH_3CN/H_2O (1:1, 2.12 mL). RP HPLC (1:99 (10 min)→35:65 (20 min)→100% H_2O with 0.1% TFA/CH_3CN), followed by lyophilization of the aqueous phases afforded the bis-TFA salt of (+)-**3** (49.9 mg, 51% over two steps). White powder; mp: 136–137 °C; $[\alpha]_D^{20} = +27$ (c = 0.5, MeOH); ^{1}H NMR (300 MHz, CD_3OD): δ = 2.96 (t, J = 6.9 Hz, 2H, H-C8), 3.36–3.47 (m, 3H, H-C9 and H_a-C5′), 3.57 (dd, J = 14.4, 7.8 Hz, 1H, H_b-C5′), 3.88 (t, J = 6.0 Hz, 1H, H-C3′), 3.95–4.01 (m, 1H, H-C4′), 4.16 (dd, J = 5.1, 3.5 Hz, 1H, H-C2′), 5.58 (d, J = 3.5 Hz, 1H, H-C1′), 6.51 (d, J = 7.8 Hz, 1H, H-C5), 7.50–7.56 (m, 2H, H-C14), 7.68–7.72 (m, 2H, H-C13), 7.89 ppm (d, J = 7.8 Hz, 1H, H-C6); ^{13}C NMR (75 MHz, CD_3OD): δ = 23.35 (C9), 32.50 (C8), 42.03 (C5′), 72.18 (C3′), 75.01 (C2′), 83.86 (C4′), 93.55 (C1′), 94.62 (C5), 114.38 (C13), 127.02 (C14), 132.06 (C12), 146.42 (C6), 148.39 (C10), 154.83 (C2), 161.19 (C4), 172.65 ppm (C7); IR (neat): $\tilde{\nu}$ = 3261w, 3075w, 2925w, 1724w, 1662s (br), 1571w, 1556w, 1541w, 1463w, 1429w (br), 1274w (br), 1188s (br), 1130s (br), 1070w, 889w, 835w, 798m, 781w, 751m, 721s cm^{-1}; HR-MALDI-MS (3-HPA): calcd for $C_{19}H_{23}N_6O_5^+$ ($[M+H]^+$): 415.1724, found: 415.1716.

2-{3-[({(2*R*,3*S*,4*R*,5*R*)-5-[4-(Butylammonio)-2-oxopyrimidin-1(2*H*)-yl]-3,4-dihydroxytetrahydrofuran-2-yl}methyl)amino]-3-oxopropyl}-1*H*-3,1-benzimidazol-1-ium bis(trifluoroacetate) ((+)-**4**): General procedure A, starting from the amine (+)-**13** (50 mg, 0.15 mmol) and Et_3N (21 μL, 0.15 mmol) in anhydrous DMF (1 mL) and commercially available **11** (28 mg, 0.15 mmol), HBTU (56 mg, 0.15 mmol), and HOBt (20 mg, 0.15 mmol) in anhydrous DMF (1.5 mL). FC (Et_3N/MeOH/AcOEt 1:10:89) afforded the protected intermediate (71 mg, 93%), which was taken directly to the next step without further characterization. General procedure B, starting from this intermediate and TFA (0.66 mL) in CH_3CN/H_2O (1:1, 2.2 mL). RP HPLC (5:99 (10 min)→35:65 (20 min)→100% H_2O with 0.1% TFA/MeCN), followed by lyophilization to afford the bis-TFA salt of (+)-**4** (41.1 mg, 39% over two steps) as a mixture two conformers denoted **A** and **B** (CD_3OD, **A**/**B** = 3:1). White powder; mp: 107–109 °C; $[\alpha]_D^{20} = +11.6$ (c = 0.5, MeOH); ^{1}H NMR (300 MHz, CD_3OD): δ = 1.00 (t, J = 7.2 Hz, 6H, H-C10), 1.39–1.51 (m, 4H, H-C9), 1.68 (qt, J = 7.2 Hz, 4H, H-C8), 2.95 (t, J = 6.9 Hz, 4H, H-C12), 3.39–3.63 (m, 12H, H-C5′, H-C7, and H-C13), 3.87–3.92 (m, 2H, H-C4′), 3.96–4.02 (m, 2H, H-C3′), 4.17 (dd, J = 5.4, 3.5 Hz, 2H, H-C2′), 5.56 (d, J = 3.3 Hz, 1H, H_B-C1′), 5.61 (d, J = 3.5 Hz, 1H, H_A-C1′), 6.00 (d, J = 7.8 Hz, 1H, H_B-C5), 6.22 (d, J = 8.1 Hz, 1H, H_A-C5), 7.50–7.56 (m, 4H, H-C18), 7.67–7.74 (m, 4H, H-C17), 7.77 (d, J = 7.8 Hz, 1H, H_A-C6), 7.98 ppm (d, J = 8.1 Hz, 1H, H_B-C6); ^{13}C NMR (75 MHz, CD_3OD): δ = 13.69 (C10), 20.70 (C13), 23.35 (C9), 30.87 (C12), 31.61 (C_B8), 32.46 (C_A8), 41.90 (C_B5′), 42.19 (C_A5′), 43.42 (C_A7), 44.02 (C_B7), 72.11 (C_B3′), 72.31 (C_A3′), 74.98 (C2′), 83.75 (C_A4′), 83.88 (C_B4′), 91.50 (C_B1′), 93.18 (C_A1′), 94.13 (C_B5), 95.45 (C_A5), 114.40 (C17), 126.99 (C18), 132.078 (C16), 143.71 (C6), 149.21 (C14), 154.85 (C2), 158.96 (C4), 172.63 ppm (C7), (13 C buried); IR (neat): $\tilde{\nu}$ = 3266w, 3090w, 2935w, 2863w, 1929w, 1662s (br), 1558w, 1463w, 1425w, 1275w, 1198s, 1186s (br), 1127s (br), 1075m, 1055m, 833m, 798m, 751m, 720s cm^{-1}; HR-MALDI-MS (3-HPA): calcd for $C_{23}H_{31}N_6O_5^+$ ($[M+H]^+$): 471.2350, found: 471.2353.

***N*⁴-Acetyl-2′,3′-*O*-isopropylidenecytidine** ((−)-**5**):[28] Triethyl orthoformate (23 mL, 140 mmol) was added dropwise over 15 min to a vigorously stirred suspension of *N*⁴-acetylcytidine (10.0 g, 35.0 mmol) and *p*-toluenesulfonic acid monohydrate (6.65 g, 35.0 mmol) in anhydrous acetone (70 mL). After 1 h, the solution became clear and was neutralized with 28% NH_4OH (aq), and the volatiles were removed in vacuo. The residue was dissolved in H_2O (100 mL) and cooled to 0 °C. After 18 h, the resulting solid precipitate was collected by filtration, washed with ice-cold H_2O, and dried to afford (−)-**5** (9.5 g, 83%). White powder; mp: 131 °C (Ref. [28]: 125–129 °C); $[\alpha]_D^{20} = -4.0$ (c = 0.5, MeOH); ^{1}H NMR (400 MHz, $(CD_3)_2SO$): δ = 1.29 (s, 3H, CH_3), 1.49 (s, 3H, CH_3), 2.10 (s, 3H, $COCH_3$), 3.54–3.59 (m, 1H, H_a-C5′), 3.62–3.67 (m, 1H, H_b-C5′), 4.20 (dd, J = 7.8, 3.8 Hz, 1H, H-C4′), 4.76 (dd, J = 6.2, 3.8 Hz, 1H, H-C3′), 4.87 (dd, J = 6.2, 2.1 Hz, 1H, H-C2′), 5.09 (t, J = 5.1 Hz, 1H, H-O5′), 5.85 (d, J = 2.1 Hz, 1H, H-C1′), 7.19 (d, J = 7.5 Hz, 1H, H-C5), 8.22 (d, J = 7.5 Hz, 1H, H-C6), 10.89 ppm (s, 1H, NHAc); ^{13}C NMR (100 MHz, $(CD_3)_2SO$): δ = 20.95 (CH_3), 24.27 (CH_3), 26.89 ($COCH_3$), 58.43 (C5′), 80.49 (C3′), 84.71 (C2′), 87.61 (C4′), 93.40 (C1′), 96.52 (C5), 112.48 ($C(CH_3)_2$), 146.41 (C6), 154.38 (C2), 162.60 (C4), 170.97 ppm (C8); HR-MALDI-MS (3-HPA): calcd for $C_{14}H_{19}N_3NaO_6^+$ ($[M+Na]^+$): 348.1166, found: 348.1170.

***N*⁴-Acetyl-5′-deoxy-5′-(1,3-dioxo-1,3-dihydro-2*H*-isoindol-2-yl)-2′,3′-*O*-(1-methylethylidene)cytidine** ((+)-**6**): DIAD (3.63 mL, 18.45 mmol) was added dropwise to a stirred suspension of (−)-**5** (3.0 g, 9.23 mmol), PPh_3 (4.83 g, 18.45 mmol), and phthalimide (2.71 g, 18.45 mmol) in anhydrous DMF (46 mL) at 20 °C. After 18 h, MeOH (10 mL) was added and the solution was stirred for an additional 1 h until the solution became clear and colorless. The volatiles were removed in vacuo. FC (AcOEt/hexanes 1:1→AcOEt) afforded (+)-**6** (2.95 g, 70%). White solid; mp: > 244 °C (dec); $[\alpha]_D^{20} = +97.3$ (c = 0.5, $CHCl_3$); ^{1}H NMR (300 MHz, $CDCl_3$): δ = 1.31 (s, 3H, CH_3), 1.50 (s, 3H, CH_3), 2.31 (s, 3H, $COCH_3$), 3.97 (dd, J = 14.1, 5.4 Hz, 1H, H_a-C5′), 4.15 (dd, J = 14.1, 8.4 Hz, 1H, H_b-C5′), 4.44–4.50 (m, 1H, H-C4′), 4.96 (dd, J = 6.6, 3.9 Hz, 1H, H-C3′), 5.17 (dd, J = 6.3, 1.2 Hz, 1H, H-C2′), 5.56 (s, 1H, H-C1′), 7.47 (d, J = 7.5 Hz, 1H, H-C5), 7.66–7.72 (m, 3H, H-C6 and H-C10), 7.79–7.82 (m, 2H, H-C9), 10.40 ppm (s, 1H, $NHCOCH_3$); ^{13}C NMR (75 MHz, $CDCl_3$): δ = 25.11 (CH_3), 25.30 (CH_3), 27.06 ($COCH_3$), 40.11 (C5′), 82.67 (C3′), 84.98 (C2′), 86.33 (C4′), 97.21 (C1′), 97.37 (C5), 113.96 ($C(CH_3)_2$), 123.25 (C9), 131.81 (C8), 133.85 (C10), 147.27 (C6), 154.73 (C2), 163.67 (C4), 167.88 (C7), 171.22 ppm ($COCH_3$); IR (neat): $\tilde{\nu}$ = 3309w, 2973w, 1788w, 1708s, 1662s, 1623m, 1549m, 1488s, 1439m, 1394s, 1317s, 1274w, 1233w, 1204s, 1155m, 1137m, 1088s, 1069s, 1039m, 1014m, 1002m, 967w, 944w, 882w, 869s, 801w, 790s, 727s, 718s cm^{-1}; HR-MALDI-MS (3-HPA): calcd for $C_{22}H_{23}N_4O_7^+$ ($[M+H]^+$): 455.1561, found: 455.1554.

5′-Deoxy-5′-(1,3-dioxo-1,3-dihydro-2*H*-isoindol-2-yl)-2′,3′-*O*-(1-methylethylidene)cytidine ((+)-**7**): A solution of 7 M NH_3/MeOH (18 mL) was added dropwise over 1 h to a stirred solution of (+)-**6** (1.46 g, 3.12 mmol) in MeOH/CH_2Cl_2 (1:1, 73 mL) at 20 °C. After 6 h, the volatiles were removed in vacuo. FC (Et_3N/MeOH/AcOEt 1:10:89) afforded (+)-**7** (1.09 g, 85%). White powder; mp: > 155 °C (dec); $[\alpha]_D^{20} = +55$ (c = 0.5, $CHCl_3$); ^{1}H NMR (300 MHz, CD_3OD): δ = 1.30 (s, 3H, CH_3), 1.46 (s, 3H, CH_3), 3.98 (dd, J = 13.8, 6.0 Hz, 1H, H_b-C5′), 4.08 (dd, J = 13.8, 7.4 Hz, 1H, H_a-C5′), 4.28–4.34 (m, 1H, H-C4′),

4.95 (dd, $J=6.2$, 3.9 Hz, 1H, H-C3′), 5.11 (dd, $J=6.2$, 1.7 Hz, 1H, H-C2′), 5.44 (d, $J=1.7$ Hz, 1H, H-C1′), 5.86 (d, $J=7.4$ Hz, 1H, H-C5), 7.60 (d, $J=7.4$ Hz, 1H, H-C6), 7.75–7.83 ppm (m, 4H, H-C9 and H-C10); ^{13}C NMR (75 MHz, CD_3OD): $\delta=25.19$ (CH_3), 27.13 (CH_3), 40.83 (C5′), 83.69 (C3′), 85.93 (C2′), 86.20 (C4′), 95.72 (C1′), 96.77 (C5), 114.65 ($C(CH_3)_2$), 123.74 (C9), 132.75 (C8), 134.92 (C10), 145.29 (C6), 157.32 (C2), 167.52 (C4), 169.06 ppm (C7); IR (neat): $\tilde{\nu}=$3341w, 3183w, 2992w, 2930w, 1773w, 1709s, 1644s, 1517m, 1488m, 1431w, 1374s, 1313w, 1282m, 1208w, 1157m, 1088s, 1057s, 1010m, 875m, 856m, 787s, 712s cm^{-1}; HR-MALDI-MS (3-HPA): calcd for $C_{20}H_{21}N_4O_6^+$ ([M+H]$^+$): 413.1456, found: 413.1445.

N^4-[Bis(4-methoxyphenyl)(phenyl)methyl]-5′-deoxy-5′-(1,3-dioxo-1,3-dihydro-2*H*-isoindol-2-yl)-2′,3′-*O*-(1-methylethylidene)cytidine ((+)-**8**): Dimethoxytrityl chloride (0.986 g, 2.9 mmol) was added to a solution of Et_3N (0.405 mL, 2.9 mmol) and (+)-**7** (1.2 g, 2.9 mmol) in anhydrous CH_2Cl_2 (5.5 mL) at 20 °C. After 1 h, the volatiles were removed in vacuo. FC (Et_3N/AcOEt 1:99) afforded (+)-**8** (1.77 g, 85%). White foam; mp: 186–188 °C (dec); $[\alpha]_D^{20}=+7.5$ ($c=$0.5, $CHCl_3$); ^{1}H NMR (300 MHz, $CDCl_3$): $\delta=1.30$ (s, 3H, CH_3), 1.48 (s, 3H, CH_3), 3.80 (s, 6H, OCH_3), 4.02–4.16 (m, 2H, H-C5′), 4.35–4.41 (m, 1H, H-C4′), 4.98 (dd, $J=6.2$, 3.6 Hz, 1H, H-C3′), 5.04 (d, $J=7.2$ Hz, 1H, H-C5), 5.20 (d, $J=6.2$ Hz, 1H, H-C2′), 5.39 (s, 1H, H-C1′), 6.84 (d, $J=8.7$ Hz, 4H, H-C13), 6.98 (d, $J=7.5$ Hz, 1H, H-C6), 7.15 (d, $J=$8.9 Hz, 4H, H-C14), 7.22–7.34 (m, 5H, Ph), 7.68–7.73 (m, 2H, H-C10), 7.80–7.84 ppm (m, 2H, H-C9); ^{13}C NMR (75 MHz, $CDCl_3$): $\delta=25.38$ (CH_3), 27.12 (CH_3), 40.39 (C5′), 55.32 (OCH_3), 70.19; 83.05 (C3′), 84.96 (C2′), 85.94 (C4′), 94.81 (C1′), 96.91 (C5), 113.54, 113.73 (C-$(CH_3)_2$), 123.23 (C9), 127.38, 128.27, 128.46, 129.84, 132.01 (C8), 133.79 (C10), 136.16, 143.47, 144.38 (C6), 154.72, 158.55 (C2), 165.80 (C4), 167.90 ppm (C7); IR (neat): $\tilde{\nu}=$2934w, 1774w, 1714w, 1652s, 1634s, 1582w, 1490s, 1463m, 1439w, 1392m, 1370 m, 1299w, 1294w, 1248s, 1209w, 1178s, 1158w, 1087m, 1055m, 1031s, 875w, 828w, 785w, 723m, 712m cm^{-1}; HR-MALDI-MS (3-HPA): calcd for $C_{41}H_{38}N_4NaO_8^+$ ([M+Na]$^+$): 737.2582, found: 737.2583.

5′-Amino-N^4-[bis(4-methoxyphenyl)(phenyl)methyl]-5′-deoxy-2′,3′-*O*-(1-methylethylidene)cytidine ((+)-**9**): *n*-Butylamine (5.5 mL, 55 mmol) was added to a solution of (+)-**8** (1.7 g, 2.38 mmol) in MeOH (32 mL), and the solution was heated at 60 °C. After 5 h, the solution was cooled to 20 °C, and the volatiles were removed in vacuo. FC (Et_3N/MeOH/AcOEt 1:10:89) afforded (+)-**9** (1.2 g, 87%). Positive ninhydrin test. White powder; mp: 172–174°; $[\alpha]_D^{20}=+31.5$ ($c=0.5$, $CHCl_3$); ^{1}H NMR (300 MHz, $CDCl_3$): $\delta=1.31$ (s, 3H, CH_3), 1.51 (s, 3H, CH_3), 3.17–3.29 (m, 2H, H-C5′), 3.79 (s, 6H, OCH_3), 4.17–4.22 (m, 1H, H-C4′), 4.98 (dd, $J=6.3$, 4.2 Hz, 1H, H-C3′), 5.06–5.10 (m, 2H, H-C2′ and H-C5), 5.28 (d, $J=2.1$ Hz, 1H, H-C1′), 6.82 (d, $J=$8.4 Hz, 4H, H-C9), 6.96 (d, $J=7.8$ Hz, 1H, H-C6), 7.13 (d, $J=8.4$ Hz, 4H, H-C10), 7.19–7.33 ppm (m, 5H, Ph); ^{13}C NMR (75 MHz, $CDCl_3$): $\delta=25.39$ (CH_3), 27.30 (CH_3), 42.25 (C5′), 55.32 (OCH_3), 70.37, 81.28 (C3′), 84.16 (C2′), 86.53 (C4′), 95.31 (C1′), 97.63 (C5), 113.58 (C7), 114.24 ($C(CH_3)_2$), 127.43, 128.29, 128.44, 129.83, 135.84, 143.97, 144.55, 155.17 (C2), 158.60 (C6), 165.90 ppm (C4); IR (neat): $\tilde{\nu}=$3200w, 1656m, 1632s, 1582w, 1491s, 1460m, 1371w, 1295w, 1248s, 1210m, 1178m, 1158m, 1083m, 1068m, 1031m, 829m, 785w, 753w, 701w cm^{-1}; HR-MALDI-MS (3-HPA): calcd for $C_{33}H_{36}N_4NaO_6^+$ ([M+Na]$^+$): 607.2527, found: 607.2529.

N^4-(*tert*-Butoxycarbonyl)-5′-deoxy-5′-(1,3-dioxo-1,3-dihydro-2*H*-isoindol-2-yl)-2′,3′-*O*-(1-methylethylidene)cytidine ((+)-**12**): Di-*tert*-butyl carbonate (0.78 mL, 3.4 mmol) in dioxane (17 mL) was added dropwise to a solution of (+)-**7** (0.7 g, 1.7 mmol) in THF (17 mL), and the mixture was heated at 70 °C. After 6 h, MeOH/H_2O (1:1, 5 mL) was added, and the volatiles were removed in vacuo. FC (AcOEt/hexanes 1:1) afforded (+)-**12** (0.779 g, 90%). White powder; mp: 192–193 °C; $[\alpha]_D^{20}=+132$ ($c=0.5$, $CHCl_3$); ^{1}H NMR (300 MHz, $CDCl_3$): $\delta=1.34$ (s, 3H, CH_3), 1.52 (s, 12H, $C(CH_3)_3$ and CH_3), 4.00 (dd, $J=13.8$, 5.0 Hz, 1H, H_a-C5′), 4.19 (dd, $J=13.8$, 7.8 Hz, 1H, H_b-C5′), 4.48 (qt, $J=5.0$ Hz, 1H, H-C4′), 4.97 (dd, $J=6.3$, 3.6 Hz, 1H, H-C3′), 5.19 (dd, $J=6.3$, 1.1 Hz, 1H, H-C2′), 5.58 (d, $J=1.1$ Hz, 1H, H-C1′), 7.23 (d, $J=7.5$ Hz, 1H, H-C5), 7.42 (s br, 1H, NHBoc), 7.65–7.70 (m, 3H, H-C6 and H-C10), 7.81–7.84 ppm (m, 2H, H-C9); ^{13}C NMR (75 MHz, $CDCl_3$): $\delta=25.37$ (CH_3), 27.09 (CH_3), 28.12 (C-$(CH_3)_3$), 40.24 (C5′), 82.71 (C3′) or ($C(CH_3)_3$), 82.90 (C3′) or ($C(CH_3)_3$), 85.07 (C2′), 86.30 (C4′), 95.05 (C1′), 97.08 (C5), 113.99 ($C(CH_3)_2$), 123.26 (C9), 131.88 (C8), 133.81 (C10), 146.43 (C6), 150.94 (C2), 154.67 ($COOC(CH_3)_3$), 162.67 (C4), 167.88 ppm (C7); IR (neat): $\tilde{\nu}=$3302w, 2977w, 1772w, 1739m, 1718s, 1672m, 1628m, 1546w, 1489m, 1432w, 1392m, 1356w, 1339w, 1321w, 1280w, 1225m, 1164m, 1142s, 1089m, 1053s, 1002w, 986m, 966m, 883m, 853m, 809m, 789s, 764m, 724m, 712s cm^{-1}; HR-MALDI-MS (3-HPA): calcd for $C_{25}H_{29}N_4O_8^+$ ([M+H]$^+$): 513.1980, found: 513.1983; Anal. calcd for $C_{25}H_{28}N_4O_8$ (512.51): C 58.59, H 5.51, N 10.93; found: C 58.74, H 5.72, N 10.73.

5′-Amino-N^4-butyl-5′-deoxy-2′,3′-*O*-(1-methylethylidene)cytidine ((+)-**13**): *n*-Butylamine (0.54 mL, 5.44 mmol) was added to a solution of (+)-**12** (0.70 g, 1.36 mmol) in EtOH (18 mL), and the solution was heated at 70 °C. After 6 h, the temperature was increased to 75 °C and stirring was continued. After an additional 2 h, the solution was cooled to 20 °C, and the volatiles were removed in vacuo. FC (Et_3N/MeOH/AcOEt 1:10:89) afforded (+)-**13** (0.375 g, 82%). Positive ninhydrin test. White foam; mp: 54–56 °C; $[\alpha]_D^{20}=+18.2$ ($c=$0.5, $CHCl_3$); ^{1}H NMR (300 MHz, CD_3OD): $\delta=0.94$ (t, $J=7.2$ Hz, 3H, H-C10), 1.28–1.46 (m, 5H, H-C9), CH_3), 1.52–1.61 (m, 5H, H-C8 and CH_3), 2.91 (d, $J=1.8$ Hz, 1H, H_a-C5′), 2.93 (d, $J=3.0$ Hz, 1H, H_b-C5′), 3.34 (q, $J=7.2$ Hz, 2H, H-C7), 4.01–4.06 (m, 1H, H-C4′), 4.75 (dd, $J=$6.6, 4.5 Hz, 1H, H-C3′), 5.02 (dd, $J=6.6$, 2.4 Hz, 1H, H-C2′), 5.67 (d, $J=2.4$ Hz, 1H, H-C1′), 5.80 (d, $J=7.5$ Hz, 1H, H-C5), 7.50 ppm (d, $J=7.5$ Hz, 1H, H-C6); ^{13}C NMR (75 MHz, CD_3OD): $\delta=13.88$ (C10), 20.85 (C9), 25.33 (CH_3), 27.30 (CH_3), 31.82 (C8), 41.11 (C5′), 44.30 (C7), 82.64 (C3′), 85.42 (C2′), 88.47 (C4′), 95.64 (C1′), 96.72 (C5), 114.88 ($C(CH_3)_2$), 143.16 (C6), 157.73 (C2), 165.14 ppm (C4); IR (neat): $\tilde{\nu}=$3266w, 3121w, 2968w, 2951w, 2931w, 1637s, 1578m, 1505s, 1465m, 1432w, 1372m, 1318w, 1279m, 1211m, 1157m, 1065s, 969w, 941w, 876w, 858m, 785s cm^{-1}; HR-MALDI-MS (3-HPA): calcd for $C_{16}H_{27}N_4O_4^+$ ([M+H]$^+$): 339.2027, found: 339.2025.

In vitro assays

Materials. [1,3,4-$^{13}C_3$]4-Diphosphocytidyl-2*C*-methyl-D-erythritol (CDP-ME) was prepared according to literature procedures.[18] *E. coli* IspE was also obtained according to published procedures.[12b] NADH and phosphoenolpyruvate potassium salt were purchased from Biomol, ATP and pyruvate kinase/lactate dehydrogenase from Sigma–Aldrich.

Enzyme-coupled photometric assay for IC_{50} determination. Assay mixtures were prepared as described[18] with some modifications: 60 μL of a solution containing 100 mM Tris-HCl (pH 8.0), 10 mM $MgCl_2$, 2 mM dithiothreitol (DTT), 2.5 mM phosphoenolpyruvate potassium salt, 2 mM ATP, 0.46 mM NADH, 1 U lactate dehydrogenase, 1 U pyruvate kinase, and IspE protein were added to 60 μL of the inhibitor solutions (final concentration varied from 16 to 2000 mM). The reaction was started by the addition of 60 μL of CDP-ME (final concentration 1 mM) and monitored at 340 nm.

Enzyme-coupled photometric assay for K_i determination. Assay mixtures were prepared as follows: 50 μL of a solution containing 100 mM Tris-HCl (pH 8.0), 10 mM $MgCl_2$, 2 mM DTT, 2.5 mM phos-

phoenolpyruvate potassium salt, 2 mM ATP, 0.46 mM NADH, 1 U lactate dehydrogenase, 1 U pyruvate kinase, and 2.4 mU IspE protein were added to 50 μL each of the inhibitor solution. The reaction was started by the addition of 50 μL CDP-ME. For the determination of each single K_M value in the presence of the inhibitor, the concentration of CDP-ME was varied from 35 to 400 mM, while keeping the concentration of the inhibitor fixed. The mixtures were incubated at 27 °C, and the reaction was monitored photometrically at 340 nm. The K_i values of the inhibitors were obtained by observing the behavior of K_M values at various inhibitor concentrations (3–50 mM) and processing the data using the program Dynafit.[19]

^{13}C NMR assay. Assay mixtures contained 100 mM Tris-HCl (pH 8.0), 10 mM $MgCl_2$, 5 mM ATP, 10% (*v*/*v*) D_2O, 2 mM DTT, 1.5 mM [1,3,4-$^{13}C_3$]CDP-ME, and 13 μg IspE protein in a volume of 500 μL. Inhibitory substances were added at final concentrations ranging from 0 to 3 mM. The mixtures were incubated at 37 °C and terminated by the addition of EDTA to a final concentration of 20 mM. The solution was analyzed by ^{13}C NMR spectroscopy on a Bruker DRX 500 (125 MHz) and referenced to an internal standard of [1-$^{13}C_1$]glucose (0.9 mM).

X-ray crystallography. Crystals of *A. aeolicus* IspE complexed with (−)-**1** and (+)-**3** were obtained by the hanging-drop vapor-diffusion method. Further details are included in the PDB depositions (PDB codes: 2V2Q and 2V2V for the co-crystal structures with (−)-**1** and (+)-**3**, respectively). The enzyme was first incubated with each ligand and AMP for 1 h at 4 °C prior to setting up drops. The reservoir solution was 1.6 M $(NH_4)_2SO_4$, 100 mM $(CH_3)_2AsO_2Na$ pH 6.5, 100 mM NaBr. The hanging drop consisted of 1 μL reservoir solution and 1 μL protein solution (30 mg mL^{-1}) in 10 mM Tris-HCl pH 8.5, 20 mM NaCl, 1 mM DTT, 4 mM AMP, and 4 mM ligand. Crystals were cryo-protected in a solution containing 20% glycerol, and data were collected on a RaxisIV^{++} image plate detector coupled to a Rigaku M007 rotating anode X-ray generator (Cu K_α, λ = 1.5418 Å), then processed using MOSFLM.[29] The crystals are cubic pyramids in the space group $P2_13$ with unit cell dimensions $a = b = c$ = 137.0 Å for the complex with (+)-**3**, and $a = b = c$ = 137.3 Å for the complex with (−)-**1**. The dataset for compound (+)-**3** was 99.9% complete to 2.3 Å resolution with an R_{sym} of 8.3%, 58.5% in the outer resolution bin. The dataset for compound (−)-**1** was 99.9% complete to 2.4 Å resolution with an R_{sym} of 8.2%, 58.1% in the outer shell. The starting model for each analysis was the previously solved *A. aeolicus* IspE structure,[24] and molecular replacement using MOLREP[30] was used to generate a model for refinement. Rigid body refinement using REFMAC5[31] preceded a combination of model building in COOT[32] and restrained refinement (REFMAC5) to an R_{factor} and R_{free} of 21.2% and 22.7% for compound (+)-**3**, 21.7% and 27.2% for compound (−)-**1**. The model for the complex with compound (+)-**3** consisted of 539 residues, 2 ligand molecules, 348 water molecules, 5 sulfate anions, 7 bromide anions, and 2 glycerol molecules; 98.0% of residues were in the most favored regions of the Ramachandran plot (MOLPROBITY)[33] with no residues in the disallowed regions. The complex with compound (−)-**1** consisted of 540 residues, 2 ligand molecules, 264 water molecules, 5 sulfate anions, 8 bromide anions, and 3 glycerol molecules; 97.5% of residues were in the most favored regions of the Ramachandran plot with 2 residues in the disallowed regions. In both cases, atoms of the cytosine moiety of the ligands were assigned full occupancy. The remaining atoms were given zero occupancy to identify that the electron density associated with them was poorly defined.

Acknowledgements

We gratefully acknowledge financial support for this work from the following agencies: ETH Research Council, the Munich Center for Integrated Protein Science, the Hans-Fischer-Gesellschaft, the Wellcome Trust (to W.N.H.), and the Biotechnology and Biological Sciences Research Council (UK) (to W.N.H.).

Keywords: crystal structure analysis · drug design · inhibitors · kinases · non-mevalonate pathway

[1] a) M. Rohmer, M. Knani, P. Simonin, B. Sutter, H. Sahm, *Biochem. J.* **1993**, *295*, 517–524; b) M. K. Schwarz, No. 10951, PhD dissertation, ETH Zurich, **1994**; c) S. T. J. Broers, No. 10978, PhD dissertation, ETH Zurich, **1994**; d) W. Eisenreich, B. Menhard, P. J. Hylands, M. H. Zenk, A. Bacher, *Proc. Natl. Acad. Sci. USA* **1996**, *93*, 6431–6436; e) W. Eisenreich, M. Schwarz, A. Cartayrade, D. Arigoni, M. H. Zenk, A. Bacher, *Chem. Biol.* **1998**, *5*, R221–R233.

[2] Y. Boucher, W. F. Doolittle, *Mol. Microbiol.* **2000**, *37*, 703–716.

[3] a) F. Rohdich, J. Wungsintaweekul, M. Fellermeier, S. Sagner, S. Herz, K. Kis, W. Eisenreich, A. Bacher, M. H. Zenk, *Proc. Natl. Acad. Sci. USA* **1999**, *96*, 11758–11763; b) F. Rohdich, S. Hecht, A. Bacher, W. Eisenreich, *Pure Appl. Chem.* **2003**, *75*, 393–405.

[4] H. Jomaa, J. Wiesner, S. Sanderbrand, B. Altincicek, C. Weidemeyer, M. Hintz, I. Türbachova, M. Eberl, J. Zeidler, H. K. Lichtenthaler, D. Soldati, E. Beck, *Science* **1999**, *285*, 1573–1576.

[5] http://www.cdc.gov/tb/WorldTBDay/resources_global.htm.

[6] a) U. Weiss, *Nature* **2002**, *415*, 669; b) J. K. Baird, *N. Engl. J. Med.* **2005**, *352*, 1565–1577; c) http://www.cdc.gov/malaria/impact/index.htm; d) M. Schlitzer, *ChemMedChem* **2007**, *2*, 944–986.

[7] a) A. L. Kritski, L. S. Rodrigues de Jesus, M. K. Andrade, E. Werneck-Barroso, M. A. Vieira, A. Haffner, L. W. Riley, *Chest* **1997**, *111*, 1162–1167; b) J. E. Ollé-Goig, *Trop. Med. Int. Health* **2006**, *11*, 1625–1628.

[8] For some selected publications on fosmidomycin and derivatives, see: a) T. Kuzuyama, T. Shimizu, S. Takahashi, H. Seto, *Tetrahedron Lett.* **1998**, *39*, 7913–7916; b) M. A. Missinou, S. Borrmann, A. Schindler, S. Issifou, A. A. Adegnika, P.-B. Matsiegui, R. Binder, B. Lell, J. Wiesner, T. Baranek, H. Jomaa, P. G. Kremsner, *Lancet* **2002**, *360*, 1941–1942; c) J. Wiesner, R. Ortmann, H. Jomaa, M. Schlitzer, *Angew. Chem.* **2003**, *115*, 5432–5451; *Angew. Chem. Int. Ed.* **2003**, *42*, 5274–5293; d) B. Lell, R. Ruangweerayut, J. Wiesner, M. A. Missinou, A. Schindler, T. Baranek, M. Hintz, D. Hutchinson, H. Jomaa, P. G. Kremsner, *Antimicrob. Agents Chemother.* **2003**, *47*, 735–738; e) S. Oyakhirome, S. Issifou, P. Pongratz, F. Barondi, M. Ramharter, J. F. Kun, M. A. Missinou, B. Lell, P. G. Kremsner, *Antimicrob. Agents Chemother.* **2007**, *51*, 1869–1871; f) N. Singh, G. Cheve, M. A. Avery, C. R. McCurdy, *Curr. Pharm. Des.* **2007**, *13*, 1161–1177.

[9] W. N. Hunter, *J. Biol. Chem.* **2007**, *282*, 21573–21577.

[10] A. K. H. Hirsch, S. Lauw, P. Gersbach, W. B. Schweizer, F. Rohdich, W. Eisenreich, A. Bacher, F. Diederich, *ChemMedChem* **2007**, *2*, 806–810.

[11] a) C. M. Crane, J. Kaiser, N. L. Ramsden, S. Lauw, F. Rohdich, W. Eisenreich, W. N. Hunter, A. Bacher, F. Diederich, *Angew. Chem.* **2006**, *118*, 1082–1087; *Angew. Chem. Int. Ed.* **2006**, *45*, 1069–1074; b) C. Baumgartner, C. Eberle, F. Diederich, S. Lauw, F. Rohdich, W. Eisenreich, A. Bacher, *Helv. Chim. Acta* **2007**, *90*, 1043–1068.

[12] a) F. Rohdich, J. Wungsintaweekul, H. Lüttgen, M. Fischer, W. Eisenreich, C. A. Schuhr, M. Fellermeier, N. Schramek, M. H. Zenk, A. Bacher, *Proc. Natl. Acad. Sci. USA* **2000**, *97*, 8251–8256; b) H. Lüttgen, F. Rohdich, S. Herz, J. Wungsintaweekul, S. Hecht, C. A. Schuhr, M. Fellermeier, S. Sagner, M. H. Zenk, A. Bacher, W. Eisenreich, *Proc. Natl. Acad. Sci. USA.* **2000**, *97*, 1062–1067; c) T. Kuzuyama, M. Takagi, K. Kaneda, H. Watanabe, T. Dairi, H. Seto, *Tetrahedron Lett.* **2000**, *41*, 2925- 2928.

[13] a) S. Herz, J. Wungsintaweekul, C. A. Schuhr, S. Hecht, H. Lüttgen, S. Sagner, M. Fellermeier, W. Eisenreich, M. H. Zenk, A. Bacher, F. Rohdich, *Proc. Natl. Acad. Sci. USA* **2000**, *97*, 2486–2490; b) F. Rohdich, W. Eisenreich, J. Wungsintaweekul, S. Hecht, C. A. Schuhr, A. Bacher, *Eur. J. Biochem.* **2001**, *268*, 3190–3197.

[14] a) Y.-H. Woo, R. P. M. Fernandes, P. J. Proteau, *Bioorg. Med. Chem.* **2006**, *14*, 2375–2385; b) V. Devreux, J. Wiesner, J. L. Goeman, J. Van der Eycken, H. Jomaa, S. Van Calenbergh, *J. Med. Chem.* **2006**, *49*, 2656–2660; c) T. Haemers, J. Wiesner, S. Van Poecke, J. Goeman, D. Henschker, E. Beck, H. Jomaa, S. Van Calenbergh, *Bioorg. Med. Chem. Lett.* **2006**, *16*, 1888–1891.

[15] a) T. Kuzuyama, M. Takagi, K. Kaneda, T. Dairi, H. Seto, *Tetrahedron Lett.* **2000**, *41*, 703–706; b) F. Rohdich, J. Wungsintaweekul, W. Eisenreich, G. Richter, C. A. Schuhr, S. Hecht, M. H. Zenk, A. Bacher, *Proc. Natl. Acad. Sci. USA* **2000**, *97*, 6451–6456; c) S. B. Richard, M. E. Bowman, W. Kwiatkowski, I. Kang, C. Chow, A. M. Lillo, D. E. Cane, J. P. Noel, *Nat. Struct. Biol.* **2001**, *8*, 641–648; d) L. E. Kemp, C. S. Bond, W. N. Hunter, *Acta Crystallogr. Sect. D* **2003**, *59*, 607–610.

[16] a) E. Sonveaux, *Methods Mol. Biol.* **1994**, *26*, 1–71; b) H. Weber, H. G. Khorana, *J. Mol. Biol.* **1972**, *72*, 219–249.

[17] P. Vicini, M. Incerti, L. Amoretti, V. Ballabeni, M. Tognolini, E. Barocelli, *Farmaco* **2002**, *57*, 363–367.

[18] V. Illarionova, J. Kaiser, E. Ostrozhenkova, A. Bacher, M. Fischer, W. Eisenreich, F. Rohdich, *J. Org. Chem.* **2006**, *71*, 8824–8834.

[19] P. Kuzmic, *Anal. Biochem.* **1996**, *237*, 260–273.

[20] T. Wada, T. Kuzuyama, S. Satoh, S. Kuramitsu, S. Yokoyama, S. Unzai, J. R. H. Tame, S.-Y. Park, *J. Biol. Chem.* **2003**, *278*, 30022–30027.

[21] L. Miallau, M. S. Alphey, L. E. Kemp, G. A. Leonard, S. M. McSweeney, S. Hecht, A. Bacher, W. Eisenreich, F. Rohdich, W. N. Hunter, *Proc. Natl. Acad. Sci. USA.* **2003**, *100*, 9173–9178.

[22] a) P. R. Gerber, K. Müller, *J. Comput.-Aided Mol. Des.* **1995**, *9*, 251–268; b) Gerber Molecular Design (http://www.moloc.ch).

[23] a) All molecular graphics images were produced using the UCSF Chimera package from the Resource for Biocomputing, Visualization, and Informatics at the University of California, San Francisco (supported by NIH P41 RR-01081); For details, see: b) E. F. Pettersen, T. D. Goddard, C. C. Huang, G. S. Couch, D. M. Greenblatt, E. C. Meng, T. E. Ferrin, *J. Comput. Chem.* **2004**, *25*, 1605–1612; c) Chimera home page can be found at http://www.cgl.ucsf.edu/chimera.

[24] T. Sgraja, M. S. Alphey, S. Ghilagaber, R. Marquez, W. N. Hunter, unpublished results.

[25] a) J. W. Pflugrath, F. A. Quiocho, *Nature* **1985**, *314*, 257–260; b) H. Luecke, F. A. Quiocho, *Nature* **1990**, *347*, 402–406; c) J. J. He, F. A. Quiocho, *Science* **1991**, *251*, 1479–1481.

[26] A. K. H. Hirsch, F. R. Fischer, F. Diederich, *Angew. Chem.* **2007**, *119*, 342–357; *Angew. Chem. Int. Ed.* **2007**, *46*, 338–352.

[27] S. M. Marcuccio, B. C. Elmes, G. Holan, E. J. Middleton, *Nucleosides Nucleotides* **1992**, *11*, 1695–1701.

[28] a) J. P. H. Verheyden, J. G. Moffatt, *J. Org. Chem.* **1974**, *39*, 3573–3579; b) K.-Y. Jung, R. J. Hohl, A. J. Wiemer, D. F. Wiemer, *Bioorg. Med. Chem.* **2000**, *8*, 2501–2509.

[29] A. G. W. Leslie, H. R. Powell, G. Winter, O. Svensson, D. Spruce, S. McSweeney, D. Love, S. Kinder, E. Duke, C. Nave, *Acta Crystallogr. Sect. D* **2002**, *58*, 1924–1928.

[30] A. Vagin, A. Teplyakov, *J. Appl. Crystallogr.* **1997**, *30*, 1022–1025.

[31] G. N. Murshudov, A. A. Vagin, E. J. Dodson, *Acta Crystallogr. Sect. D* **1997**, *53*, 240–255.

[32] P. Emsley, K. Cowtan, *Acta Crystallogr. Sect. D* **2004**, *60*, 2126–2132.

[33] S. C. Lovell, I. W. Davis, W. B. Arendall III, P. I. W. de Bakker, J. M. Word, M. G. Prisant, J. S. Richardson, D. C. Richardson, *Proteins: Struct. Funct. Gen.* **2003**, *50*, 437–450.

Received: August 13, 2007
Published online on November 21, 2007

